

High-Resolution Fourier Transform and Submillimeter-wave Study of the ν_6 Band of $^{12}\text{CH}_3\text{F}$

D. PAPOUŠEK, R. TESAŘ, AND P. PRACNA

J. Heyrovský Institute of Physical Chemistry and Electrochemistry, Czechoslovak Academy of Sciences, Dolejškova, 182 23 Prague 8, Czechoslovakia

S. CIVIŠ¹ AND M. WINNEWISSER

Physikalisch-Chemisches Institut, Justus-Liebig-Universität Giessen, Heinrich-Buff-Ring 58, D-6300 Giessen, Federal Republic of Germany

AND

S. P. BELOV AND M. YU. TRETYAKOV

Institute of Applied Physics, Academy of Sciences of the USSR, Uljanov Street 46, 603600 Nizhnii Novgorod, USSR

The ν_6 band of $^{12}\text{CH}_3\text{F}$ has been measured in the range 1077–1278 cm^{-1} using a Fourier transform spectrometer with a resolution of 0.002 cm^{-1} . The wavenumbers of 1070 rovibrational transitions have been used simultaneously with 99 previously reported frequencies of the ground state rotational transitions and 135 frequencies of rotational transitions in the $\nu_6 = 1$ excited vibrational state to determine 24 parameters of the ν_6 band and 6 spectroscopic parameters of the ground vibrational state of $^{12}\text{CH}_3\text{F}$. © 1991 Academic Press, Inc.

I. INTRODUCTION

The ν_6 band of $^{12}\text{CH}_3\text{F}$ consists of the $\Delta\nu_6 = 1$, $\Delta J = 0, \pm 1$, $\Delta K = \pm 1$ rovibrational transitions to the doubly degenerate vibrational level of the CH_3 rocking mode. Smith and Mills (1) recorded this band with 0.25- cm^{-1} resolution, resolved partly the J and K structure of the band, and observed intensity perturbations in the rotational lines.

The first high-resolution study of this band was the diode laser measurement of five Q branches, done by Hirota (2). Cho *et al.* (3) used the infrared-microwave sideband laser spectrometer to measure the $\nu_3 + \nu_6 - \nu_6$ band of $^{12}\text{CH}_3\text{F}$ and determined the spectroscopic parameters of the $\nu_6 = 1$ state from about 200 transitions with J and K values up to 20 and 10, respectively.

In this paper, we report the measurement and analysis of the high-resolution Fourier transform spectra of the ν_6 band of $^{12}\text{CH}_3\text{F}$, recorded at Doppler limited resolution with the Bruker IFS 120 HR spectrometer at the University of Giessen (4). We have

¹ Present address: J. Heyrovský Institute of Physical Chemistry and Electrochemistry, Dolejškova 3, 182 23 Praha 8, Czechoslovakia.

also measured pure rotational transition frequencies in the ground and $\nu_6 = 1$ vibrational states of $^{12}\text{CH}_3\text{F}$ using the submillimeter-wave RAD3 spectrometer with acoustic detection which was built at the Institute of Applied Physics in Nizhnii Novgorod (formerly Gorkii) (5).

The ν_6 band of $^{12}\text{CH}_3\text{F}$ is an ideal example for testing different reduction schemes of effective rotational Hamiltonians developed for degenerate vibrational states of symmetric top molecules (6–8) which are not strongly perturbed by Coriolis interactions with other vibrational states. This is a problem of the determinability of various spectroscopic parameters in the effective rotational Hamiltonians, which will be discussed in more detail in Sections III and IV of this paper.

Last but not least, methyl fluoride has been used for various laser spectroscopic experiments [see, e.g., Ref. (9) and the references cited therein] and for experiments with optically pumped submillimeter-wave lasers [see, e.g., Ref. (10)]. These experiments were based on the near coincidence of methyl fluoride ν_3 band transition frequencies with CO_2 laser frequencies. The data base of the precise line positions of the ν_6 band may be useful for extending these studies to another spectral region.

II. EXPERIMENTAL DETAILS

The sample of $^{12}\text{CH}_3\text{F}$ was prepared by the reaction of the methyl ester of perfluorosulfonic acid with NaF according to Edgell and Parts (11). Methyl fluoride was obtained by distillation at the temperature of a bath of solid CO_2 and ethyl alcohol as a fraction with the boiling point -78°C . Its purity was checked by the GC-MS technique.

The Fourier transform spectrum of the ν_6 band was measured with the Bruker IFS 120 HR spectrometer. The sample pressure was 50 Pa (≈ 0.375 Torr) and the path length was 284 cm at a temperature of 300 K.

After finishing the CH_3F measurement, the cell of the Bruker IFS 120 HR spectrometer was evacuated and the N_2O spectrum was measured at 50 Pa in the range $1130\text{--}1220\text{ cm}^{-1}$. Ten lines of the N_2O band were chosen in this range for calibration purposes; i.e., a correction factor was determined by fitting the differences between the measured N_2O line positions and those given in Ref. (12). The measured CH_3F line positions were then multiplied by this factor to obtain corrected line positions. The signal to noise ratio was determined to be 70.

The frequencies of the pure rotational transitions in the $\nu_6 = 1$ state of $^{12}\text{CH}_3\text{F}$ were measured with the RAD spectrometer (5) at room temperature and at sample pressures varying from 25 to 50 Pa.

III. THEORY

Energy Levels

In this paper, we will treat the ν_6 band of $^{12}\text{CH}_3\text{F}$ as an isolated band; i.e., we will assume that all the vibration–rotation interactions off-diagonal in the principle vibrational quantum numbers ν_i can be described by the effective values of spectroscopic parameters of the $\nu_6 = 1$ state (13). The expression for the rovibrational term values can be then written as

$$\begin{aligned}
E_v(J, K; l)/hc = & E_v^0/hc + B_6 J(J+1) + (A_6 - B_6)K^2 \\
& + [-2(A\zeta^z)_6 Kl + \eta_J J(J+1)Kl + \eta_K K^3 l + \tau_J J^2(J+1)^2 Kl \\
& + \tau_{JK} J(J+1)K^3 l + \tau_K K^5 l + \sigma_J J^3(J+1)^3 Kl + \sigma_{JK} J^2(J+1)^2 K^3 l \\
& + \sigma_{KJ} J(J+1)K^5 l + \sigma_K K^7 l + \dots] \\
& + \{D_J J^2(J+1)^2 - D_{JK} J(J+1)K^2 - D_K K^4 + H_J J^3(J+1)^3 \\
& + H_{JK} J^2(J+1)^2 K^2 + H_{KJ} J(J+1)K^4 + H_K K^6 \\
& + L_J J^4(J+1)^4 + L_{JK} J^3(J+1)^3 K^2 + L_{JK} J^2(J+1)^2 K^4 \\
& + L_{KKJ} J(J+1)K^6 + L_K K^8 + \dots\} + E_{\text{off-d}}/hc, \quad (1)
\end{aligned}$$

where $l = +1$ for the $+l$ levels and $l = -1$ for the $-l$ levels of the $\nu_6 = 1$ state.

The term $E_{\text{off-d}}/hc$ represents corrections to the rovibrational term value due to the terms in the expanded Hamiltonian of a C_{3v} molecule which are diagonal in v but off-diagonal in l . $E_{\text{off-d}}$ consists of several terms; the most important are considered here [cf. Ref. (14)].

(i) The $\Delta l = \pm 2$, $\Delta k = \pm 2$ interaction ("2,2" l -type interaction) has a diagonal contribution to the $kl = +1$ level of the $\nu_6 = 1$ state:

$$\begin{aligned}
\langle A_{\pm}^{(1)} | (H_{22} + H_{24})/hc | A_{\pm}^{(1)} \rangle & [\equiv E_l(J, kl = 1)/hc] \\
& = \pm 2[(q_{22} + 2f_{22}^{(K)}) + f_{22}^{(J)} J(J+1)]J(J+1), \quad (2)
\end{aligned}$$

where, using the basis functions $|v^l; J, k\rangle$,

$$|A_{\pm}^{(1)}\rangle = 2^{-1/2}[|1^{+1}; J, +1\rangle \pm |1^{-1}; J, -1\rangle]. \quad (3)$$

This interaction has the following off-diagonal contribution to the $kl \neq 1$ levels, as obtained by a second-order perturbation treatment:

$$\begin{aligned}
E_l(J, K \pm 1; \pm l) = & \pm[(q_{22} + 2f_{22}^{(K)}) + f_{22}^{(J)} J(J+1) + 2f_{22}^{(K)} K^2] \\
& \times [J(J+1) - K(K+1)][J(J+1) - K(K-1)]/[A_6 - B_6 - (A\zeta^z)_6]K, \quad (4)
\end{aligned}$$

where all the signs on both sides of this equation are correlated.

In deriving these results, we used the same phase convention for the wavefunctions as Di Leonardo *et al.* (14) in their expressions for the matrix elements of various higher-order terms in the expanded rovibrational Hamiltonian.

(ii) The $\Delta l = \pm 2$, $\Delta k = \mp 4$ interaction has the following diagonal contribution to the $kl = -2$ levels in the $\nu_6 = 1$ state:

$$\langle A_{\pm}^{(2)} | H_{24}/hc | A_{\pm}^{(2)} \rangle = \pm 2[f_{24} + f_{24}^{(J)} J(J+1)][J(J+1) - 2][J(J+1)], \quad (5)$$

where

$$|A_{\pm}^{(2)}\rangle = 2^{-1/2}[|1^{+1}; J, -2\rangle \pm |1^{-1}; J, +2\rangle]. \quad (6)$$

This interaction leads to the A_1 - A_2 splitting of the $kl = -2$ levels which was resolved for high J values in the ${}^P P_3(J)$, ${}^P Q_3(J)$, and ${}^P R_3(J)$ branches of the ν_6 band (Fig. 1).

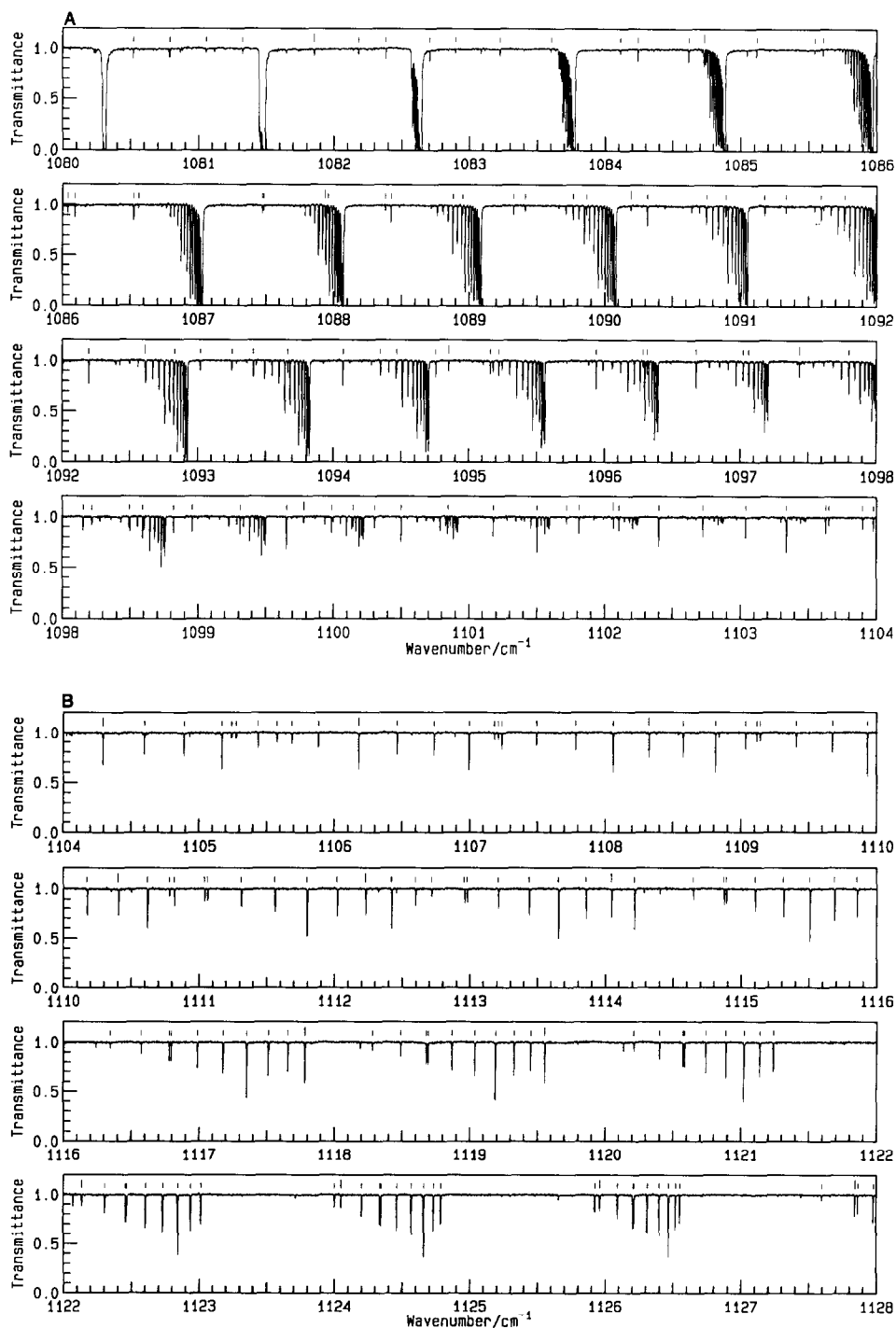


FIG. 1. Plot of the FT-IR spectrum of the ν_6 band of $^{12}\text{CH}_3\text{F}$ between 1080 and 1272 cm^{-1} . Vertical lines above the spectrum denote assigned transitions of this band, and longer lines correspond to transitions whose numbers in the list (see Table A1) are multiples of 10.

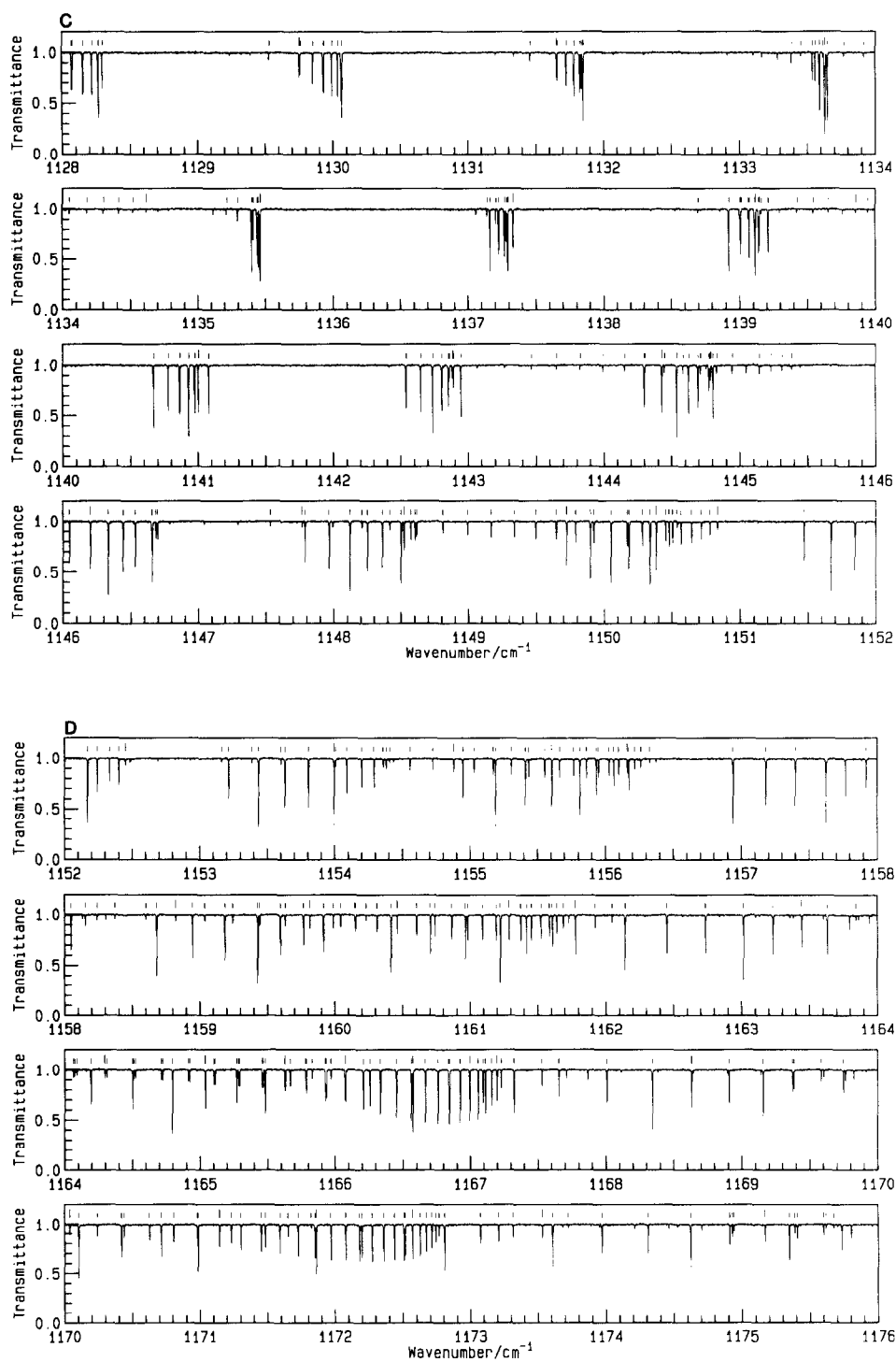


FIG. 1—Continued

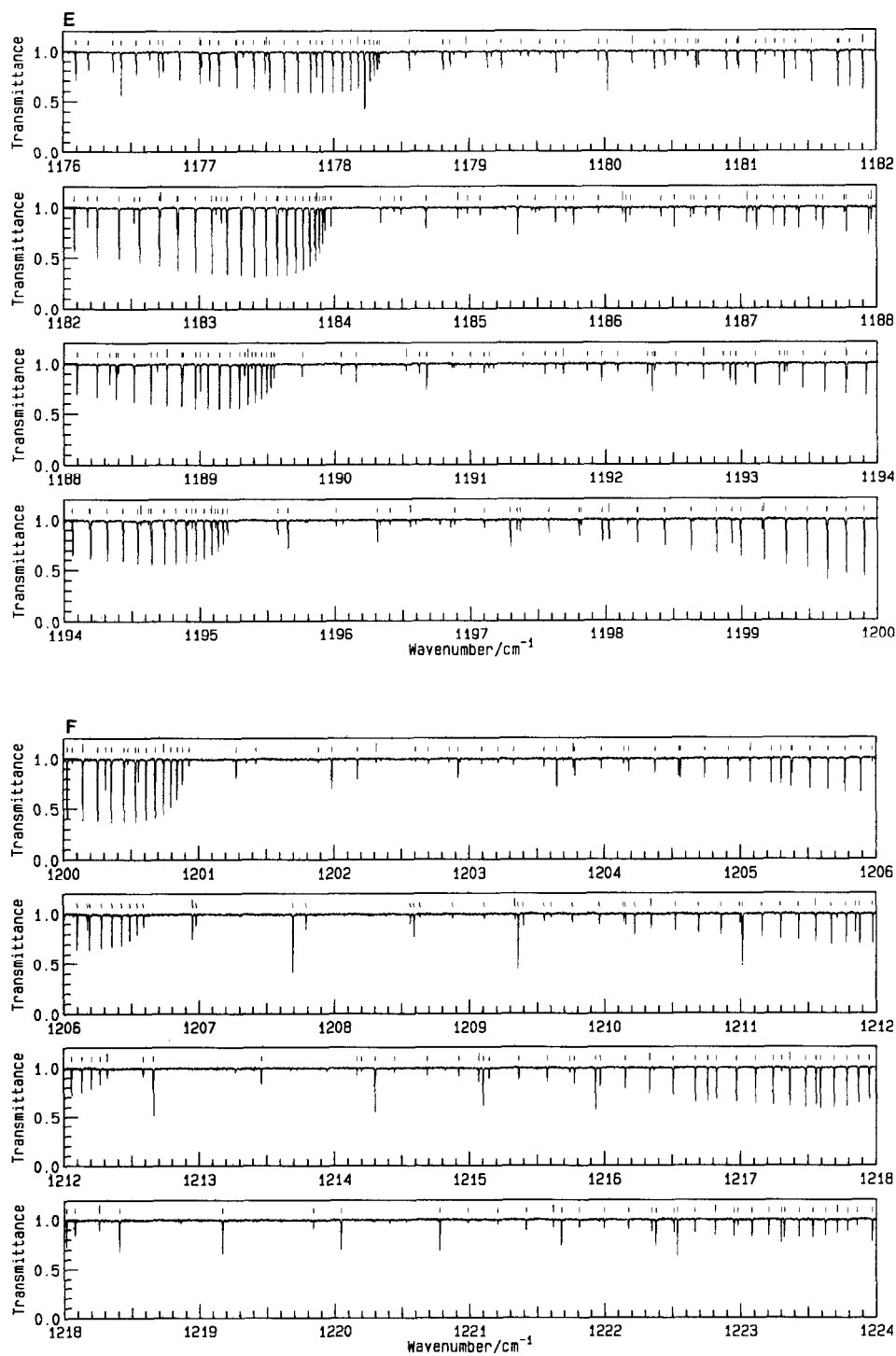


FIG. 1—Continued

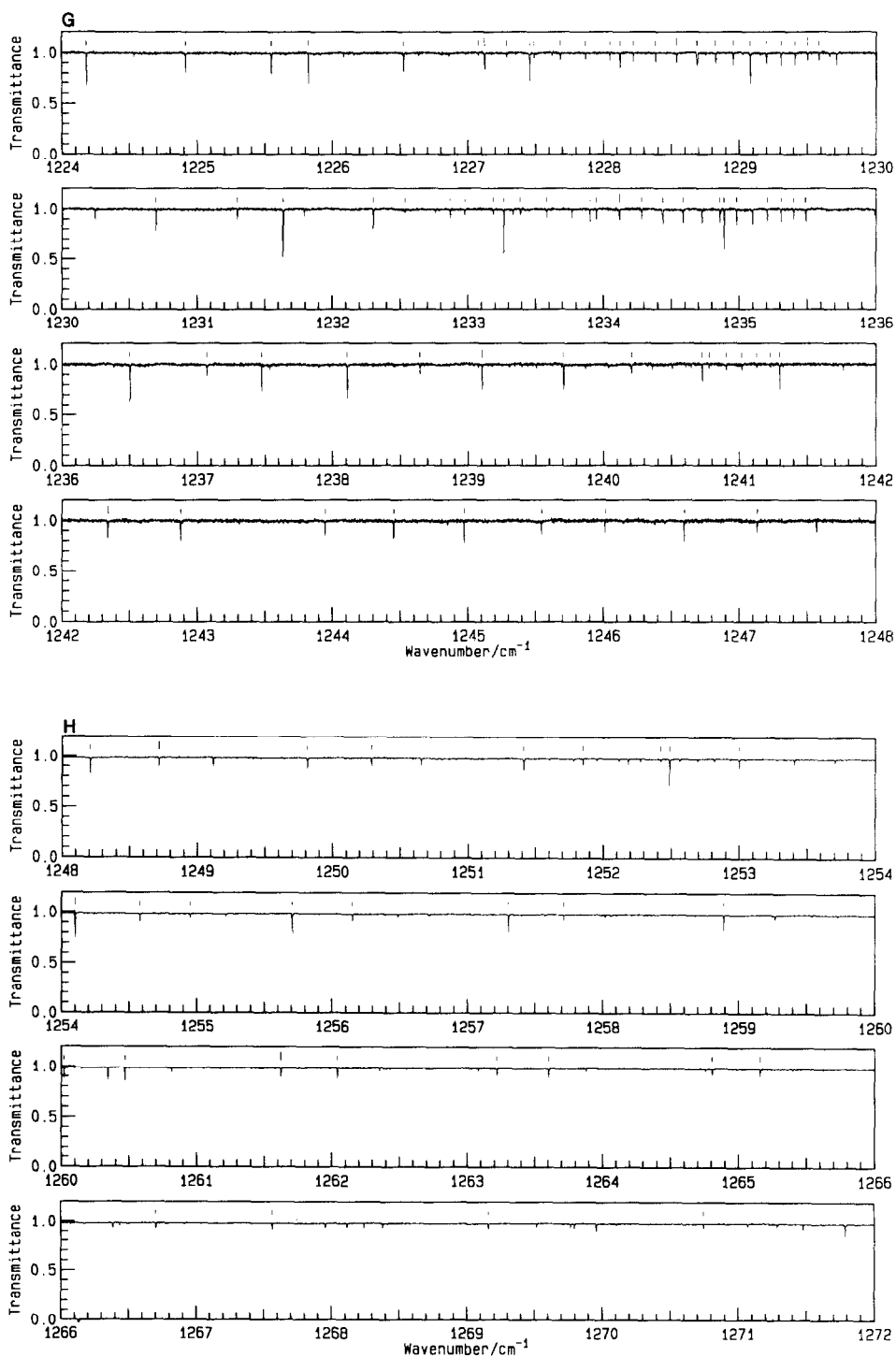


FIG. 1—Continued

On the other hand, the contribution of the off-diagonal matrix elements of this interaction was found to be negligible even for the microwave accuracy of the experiment.

(iii) The $\Delta l = \pm 2$, $\Delta k = \mp 1$ interaction (the "2,-1" l -type interaction) has purely off-diagonal contributions to the term values due to the matrix elements

$$\langle 1^{-1}; J, k+1 | (H_{22} + H_{24})/hc | 1^{+1}; J, k \rangle = 2 \{ [q_{12} + f_{12}^{(J)} J(J+1)] \times (2k+1) + f_{12}^{(K)} [k^3 + (k+1)^3] \} [J(J+1) - k(k+1)]^{1/2}. \quad (7)$$

The parameters q_{12} and $f_{12}^{(J)}$ can be shown to be completely correlated with other parameters [cf. Ref. (8)] and cannot be determined by fitting the experimental data.

The $\Delta v = \Delta l = 0$, $\Delta k = \pm 3$ interactions [ϵ parameters in Table II of Ref. (14)] are extremely small in the ground and $v_6 = 1$ states of $^{12}\text{CH}_3\text{F}$ and have not been taken into account in this paper. Thus if we put $E_v^0 = 0$, $E_{\text{off-d}} = 0$, and $l = 0$ in Eq. (1), we obtain the expression for the ground state energy levels of $^{12}\text{CH}_3\text{F}$.

Line Positions

If we apply the usual selection rules $\Delta J = 0, \pm 1$ and $\Delta K = \pm 1$ for $\Delta l = \pm 1$ transitions, employ Eq. (1), and collect terms with the same J , K , and l dependence, we obtain expressions for the wavenumbers ν of the rovibrational transitions in terms of the new effective parameters X^* .

$$\begin{aligned} \nu_{vr}(J, K; \Delta l) = & E_v^* + B_6^* J'(J'+1) + (A_6 - B_6)^* K^2 \\ & + [-2(A_5^*)_6^* Kl + \eta_J^* J'(J'+1)Kl + \eta_K^* K^3l + \tau_J^* J'^2(J'+1)^2Kl \\ & + \tau_{JK}^* J'(J'+1)K^3l + \tau_K^* K^5l + \sigma_J^* J'^3(J'+1)^3Kl \\ & + \sigma_{JK}^* J'^2(J'+1)^2K^3l + \sigma_{KJ}^* J'(J'+1)K^5l + \sigma_K^* K^7l + \dots] \\ & + [-D_J^* J'^2(J'+1)^2 - D_{JK}^* J'(J'+1)K^2 - D_K^* K^4 + H_J^* J'^3(J'+1)^3 \\ & + H_{JK}^* J'^2(J'+1)^2K^2 + H_{KJ}^* J'(J'+1)K^4 + H_K^* K^6 \\ & + L_J^* J'^4(J'+1)^4 + L_{JK}^* J'^3(J'+1)^3K^2 + \dots] \\ & + \Delta E_l^*(J', K)/hc - E_{\text{GS}}(J'', K)/hc. \quad (8) \end{aligned}$$

The parameters X^* are related to those in Eq. (1) as shown in Table I.

In Eq. (8), J' is given by $J'' + 1$ for the $\Delta J = +1$ transitions, by J'' for the $\Delta J = 0$ transitions, and by $J'' - 1$ for the $\Delta J = -1$ transitions; $l = +1$ for $\Delta K = +1$ and $l = -1$ for $\Delta K = -1$ transitions; E_{GS} is the ground state energy (J'' and K are the ground state rotational quantum numbers).

For $kl = +1$, $\Delta E_l^*(J', kl = +1)$ is

$$\Delta E_l^*(J', kl = +1)/hc = \pm 2 [q_{22}^* + f_{22}^{(J)} J'(J'+1)] J'(J'+1), \quad (9)$$

where for $q_{22}^* > 0$, the lower sign holds for $\Delta J = 0$ transitions, and the upper sign holds for the $\Delta J = \pm 1$ transitions.

For $kl \neq +1$, we have

TABLE I
Determinable Combinations of Spectroscopic Parameters of the ν_6 Band^a

| Parameter X^* | ΣX_1 | Parameter X^* | ΣX_1 |
|---------------------|--|-----------------|---|
| $E_v^* (= \nu_6^*)$ | $E_v^0 + (A_6 - B_6) - 2(A_6^2)_6 - D_K + H_K + \eta_K + \tau_K + L_K + \sigma_K$ | L_K^* | L_K |
| B_6^* | $B_6 - D_{JK} + H_{KJ} + \eta_J + \tau_{JK} + L_{KKJ} + \sigma_{KJ}$ | η_J^* | $\eta_J - 2 D_{JK} + 4 H_{KJ} + 3 \tau_{JK} + 6 L_{KKJ} + 5 \sigma_{KJ} - 2 \left((q_{22}^*)^2 + q_{22}^{(J)} f_{22}^{(J)} \right) / \alpha$ |
| D_J^* | $D_J - H_{JK} - \tau_J - L_{JK} - \sigma_{JK}$ | η_K^* | $\eta_K - 4 D_K + 20 H_K + 10 \tau_K + 56 L_K + 35 \sigma_K + (q_{22}^*)^2 / \alpha$ |
| D_{JK}^* | $D_{JK} - 6 H_{KJ} - 3 \tau_{JK} - 15 L_{KKJ} - 10 \sigma_{KJ}$ | τ_J^* | $\tau_J + 2 H_{JK} + 4 L_{JK} + 3 \sigma_{JK} + 4 \left(q_{22}^{(K)} f_{22}^{(K)} - q_{22}^{(J)} f_{22}^{(J)} \right) / \alpha$ |
| D_K^* | $D_K - 15 H_K - 5 \tau_K - 70 L_K - 35 \sigma_K$ | τ_{JK}^* | $\tau_{JK} + 4 H_{KJ} + 20 L_{KKJ} + 10 \sigma_{KJ} - 2 \left(4 q_{22}^{(K)} f_{22}^{(K)} - q_{22}^{(J)} f_{22}^{(J)} \right) / \alpha$ |
| H_J^* | $H_J + L_{JJK} + \sigma_J$ | τ_K^* | $\tau_K + 6 H_K + 56 L_K + 21 \sigma_K$ |
| H_{JK}^* | $H_{JK} + 6 L_{JK} + 3 \sigma_{JK}$ | σ_J^* | $\sigma_J + 2 L_{JJK}$ |
| H_{KJ}^* | $H_{KJ} + 15 L_{KKJ} + 5 \sigma_{KJ}$ | σ_{JK}^* | $\sigma_{JK} + 4 L_{JK}$ |
| H_K^* | $H_K + 28 L_K + 7 \sigma_K$ | σ_{KJ}^* | $\sigma_{KJ} + 6 L_{KKJ}$ |
| $(A_6 - B_6)^*$ | $(A_6 - B_6) - 6 D_K + 15 H_K + 3 \eta_K + 10 \tau_K + 28 L_K + 21 \sigma_K$ | σ_K^* | $\sigma_K + 8 L_K$ |
| $2(A_6^2)_6^*$ | $2(A_6^2)_6 - 2(A_6 - B_6) + 4 D_K - 6 H_K - 3 \eta_K - 5 \tau_K - 8 L_K + 7 \sigma_K + (q_{22}^*)^2 / \alpha^b$ | q_{22}^* | $q_{22} + 2 f_{22}^{(K)}$ |
| L_J^* | | $f_{22}^{(J)*}$ | $f_{22}^{(J)}$ |
| L_{JJK}^* | | f_{24}^* | f_{24} |
| L_{JK}^* | | $f_{24}^{(J)*}$ | $f_{24}^{(J)}$ |
| L_{KKJ}^* | | | |

^a $X^* = \sum_{i=1}^n X_i$. ^b $\alpha = A_6 - B_6 - (A_6^2)_6$.

$$\Delta E_l^*(J', kl \neq +1)/hc$$

$$= \pm [q_{22}^* + f_{22}^{(J)} J(J+1)]^2 [J(J+1)]^2 / [A_6 - B_6 - (A\zeta^z)_6] K, \quad (10)$$

where the upper sign holds for the $\Delta K = +1$ transitions and the lower sign holds for the $\Delta K = -1$ transitions.

The parameter $f_{22}^{(K)}$ is completely correlated with other spectroscopic parameters; we used therefore $f_{22}^{(K)} = 0$ [cf. Ref. (8)] in fitting the data. The values of q_{12} and $f_{12}^{(J)}$ were constrained to zero for the same reason. The parameter $f_{12}^{(K)}$ can in principle be determined but we found its value to be so small for the ν_6 band that it could not be determined from the available data.

On the other hand, the $\Delta l = \pm 2$, $\Delta k = \mp 4$ interaction leads to a measurable splitting of the $kl = -2$ levels in the ν_6 band of $^{12}\text{CH}_3\text{F}$ (Fig. 1), from which it was possible to determine $|f_{24}|$, $|f_{24}^{(J)}|$ and the relative sign of f_{24} and $f_{24}^{(J)}$ (Table III).

The $\Delta J = +1$, $\Delta K = 0$, $\Delta l = 0$ selection rules for the pure rotational transitions in the $\nu_6 = 1$ state give the following expression for the transition frequencies ν_{rot} in terms of the determinable parameters (given in cm^{-1}):

$$\begin{aligned} \nu_{\text{rot}}/c = & 2B_6^*(J+1) + \{-4D_J^*(J+1)^3 - 2D_{JK}^*(J+1)(Kl-1)^2 \\ & + H_J^*(J+1)^3[(J+2)^3 - J^3] + 4H_{JK}^*(J+1)^3(Kl-1)^2 \\ & + 2H_{KJ}^*(J+1)(Kl-l)^4 + \dots\} + [2\eta_J^*(J+1)(Kl-1) \\ & + 4\tau_J^*(J+1)^3(Kl-1) + 2\tau_{JK}^*(J+1)(Kl-1)^3 \dots] + \Delta\nu, \quad (11) \end{aligned}$$

where the expression for $\Delta\nu$ depends on kl ; for $kl = +1$, the diagonal contribution of the 2,2 l -type operator,

$$\Delta\nu_d = \pm 4[q_{22}^*(J+1) + 2f_{22}^{(J)}(J+1)^3], \quad (12)$$

gives a splitting of the rotational spectrum lines while for $kl \neq +1$, the off-diagonal effect of this interaction causes a shift of the line positions by

$$\Delta\nu_{\text{off-d}} = [|\Delta E_l^*(J+1, kl)| - |\Delta E_l^*(J, kl)|]/hc, \quad (13)$$

where ΔE_l^* is defined by Eq. (10).

For $kl = -2$, the diagonal contribution of the $\Delta l = \pm 2$, $\Delta k = \mp 4$ interaction gives

$$\Delta\nu_2 = \pm 4[2f_{24} + 3f_{24}^{(J)}(J+1)^2](J+1)(J+2). \quad (14)$$

IV. RESULTS

We have fitted separately the ground state (9, 15–17) and $\nu_6 = 1$ rotational transition frequencies (17–20), the rovibrational ν_6 line positions, and simultaneously all the rotational and rovibrational line positions. In each of these least-squares adjustments of the spectroscopic parameters, the results of which are given in Tables II and III, each transition was weighted by the inverse square of its experimental uncertainty. The uncertainty of the isolated and symmetric rovibrational line positions was estimated to be $3 \times 10^{-5} \text{ cm}^{-1}$. The uncertainties of the rotational transition frequencies in the ground state were taken from Refs. (9, 15–17), those for the $\nu_6 = 1$ state are indicated in Table A2.

Calculated and experimental values of the ν_6 band rovibrational line positions are compared in Table A1. Parameters which are obtained by a transformation inverse to that which is given in Table I are given in Table IV. They were calculated from the values of the parameters given in column II of Table III. The spectroscopic parameters in Table III and the line positions given in Table A1 are the most precise physical quantities for the ν_6 band of $^{12}\text{CH}_3\text{F}$ which have been obtained so far. Up to $J \leq 20$, the smoothed values of the wavenumbers could be used as a suitable calibration standard with better than 10^{-4} cm^{-1} accuracy. There is, however, a point which requires further work, namely, the systematic differences of the order of magnitude 10^{-4} cm^{-1} between the calculated and observed wavenumbers which appear for $J > 20$ and have opposite signs for $\Delta K = +1$ and $\Delta K = -1$ transitions (see Tables A1 and A2). We have not been able to remove them by introducing some other higher-order terms in the fit. It seems that one should take into account explicitly the x - y Coriolis interaction between $v_3 = 1$ and $v_6 = 1$ vibrational levels in order to arrive at a quantitative fit of the data for the high J values. The x - y Coriolis interaction between the $v_6 = 1$ and $v_2 = 1$ vibrational levels ($v_2 = 1$ level interacts strongly also with the $v_5 = 1$ level) might also be expected to be responsible for this effect.

This neglected interaction is probably the reason why we have larger standard errors for the ground state parameters obtained by fitting our data for the ν_6 band than those

TABLE II
Ground State Parameters of $^{12}\text{CH}_3\text{F}$ (in MHz Units)

| Parameter | I ^a | II ^b | III ^c | IV ^d |
|----------------------|--------------------------------|---------------------|--------------------|-----------------|
| A | - | 155 352.8 | 155 352.8 | - |
| B | 25 536.14965 (26) ^e | 25 536.16198 (2144) | 25 536.15010 (133) | 25 536.1499 (6) |
| $D_J \times 10^3$ | 60.23184 (142) | 60.23662 (2394) | 61.22715 (576) | 60.2330 (36) |
| $D_{JK} \times 10^3$ | 439.6000 (144) | 440.6961 (1627) | 439.6911 (661) | 439.5743 (312) |
| $D_K \times 10^3$ | - | 2108. | 2108. | - |
| $H_J \times 10^6$ | -0.0210 (22) | -0.0275 (86) | -0.0301 (58) | -0.0218 (68) |
| $H_{JK} \times 10^6$ | 1.7765 (276) | 2.5104 (11655) | 1.8785 (940) | 1.7518 (758) |
| $H_{KJ} \times 10^6$ | 21.7613 (862) | 29.7281 (207302) | 21.9731 (4228) | 21.6679 (1921) |

^aOur fit to the ground state rotational transition frequencies taken from Refs. (9, 15-17). No. of data : 99, standard deviation of the fit : 0.016 MHz.

^bFit to the transition wavenumbers of the ν_6 band. The ground state parameters A and D_K were fixed to the values given by Graner (21).

^cSimultaneous fit to all microwave, submillimeterwave, and ν_6 band transition line positions.

^dFrom Ref. (9), fit to the $v_3 = 0$ and $v_3 = 1$ rotational and ν_3 band vib-rot line positions.

^eFigures in parentheses are standard errors in units of the last digit quoted.

TABLE III
Parameters of the ν_6 Band of $^{12}\text{CH}_3\text{F}$ (in cm^{-1})

| Parameter X^a | I^a | II^b | III^c | Parameter X^a | I^a | II^b | III^c |
|-----------------------------|------------------------------|-------------------|-------------------|-------------------------------|----------------|----------------|-----------------|
| $E_v (= \nu_6)$ | 1183.93966 (15) ^d | 1183.93989 (12) | - | $\eta_k \times 10^6$ | -219.202 (177) | -219.552 (128) | - |
| B_6 | 0.847904911 (750) | 0.847904371 (114) | 0.847903938 (265) | $\tau_j \times 10^9$ | 2.626 (119) | 2.594 (100) | 3.012 (227) |
| $D_j \times 10^6$ | 2.02400 (76) | 2.02363 (25) | 2.01529 (355) | $\tau_{JK} \times 10^9$ | 15.781 (800) | 18.474 (511) | 19.387 (567) |
| $D_{JK} \times 10^6$ | 15.39635 (5922) | 15.31957 (939) | 15.31404 (128) | $\tau_k \times 10^9$ | -9.85 (185) | -10.17 (112) | - |
| $D_k \times 10^6$ | 72.6734 (354) | 72.4870 (251) | - | $\sigma_j \times 10^{13}$ | -3.034 (838) | -2.228 (732) | - |
| $H_j \times 10^{10}$ | - | - | -0.280 (141) | $\sigma_{JK} \times 10^{13}$ | 178.18 (1127) | 145.21 (722) | - |
| $H_{JK} \times 10^{10}$ | -0.704 (503) | -1.222 (218) | -1.482 (503) | $q_{22} \times 10^6$ | -73.1553 (535) | -73.1603 (481) | -73.5081 (1811) |
| $H_{KJ} \times 10^{10}$ | 14.755 (7675) | 1.641 (935) | - | $f_{22}^{(J)} \times 10^8$ | 1.80727 (715) | 1.80820 (637) | 1.92007 (9005) |
| $\Delta H_K \times 10^{10}$ | 10.367 (2106) | 0.866 (1734) | - | $f_{24}^{(J)} \times 10^{10}$ | -70.370 (1936) | -70.370 (1867) | - |
| $(A_6 - B_6)^*$ | 4.35002452 (164) | 4.35001746 (123) | - | $f_{24}^{(J)} \times 10^{13}$ | 4.98 (233) | 4.98 (224) | - |
| $2(A_6^x)_6^*$ | -5.61575815 (510) | -5.61576225 (424) | - | Type of data | No. Data | St. dev. | No. Data |
| $L_{JJK} \times 10^{12}$ | 0.0496 (178) | 0.0408 (145) | - | Ground st. rot. | - | - | 99 |
| $L_{JK} \times 10^{12}$ | -1.968 (191) | -1.289 (118) | - | Upper st. rot. | - | - | 135 |
| $L_{KKJ} \times 10^{12}$ | -3.948 (655) | 0.286 (431) | - | Vib - rot | 1070 | 3.58 MHz | 1070 |
| $\eta_j \times 10^6$ | 5.6225 (483) | 5.6013 (385) | 5.5667 (485) | | | | |

^aFit to our FTS line positions of the ν_6 band. The ground state parameters A_0 and D_0^k were fixed to the values given by Graner (21) (see Table II).

^bSimultaneous fit to the rovibrational wavenumbers, ground and $v_6 = 1$ state rotational transition frequencies.

^cFit to the upper state pure rotational frequencies [cf. Ref. (20)].

^dFigures in parentheses are standard errors in units of the last digit quoted.

obtained by Lee *et al.* (9) from the ν_3 band of $^{12}\text{CH}_3\text{F}$ (Table II). We could, of course, improve the ground state parameters by using combination differences from the ν_6 band. However, we have remeasured with Doppler-limited resolution the ν_3 band and the ν_2 , ν_5 bands of $^{12}\text{CH}_3\text{F}$, where we have been able to assign a number of forbidden vibration-rotation transitions. Furthermore, we have measured more than 200 pure rotational transitions in the $v_2 = 1$ and $v_5 = 1$ vibrational states (22).

We plan to process simultaneously all these data taking into account various rovibrational interactions using a variational approach, which should lead to precise ground state as well as the ν_3 , ν_6 , ν_2 , and ν_5 parameters.

The fact that an effective Hamiltonian describes experimental data less precisely for higher values of J is of course related to its theoretical accuracy. Badaqui and Champion (23) have proposed to weight data in merged fits such that the weights reflect not only the experimental precision $\Delta\sigma_i$ but also the theoretical accuracy of the model $\{w_i(J) = [(\Delta\sigma_i)^2 + \alpha^2 J^8]^{-1}\}$. There is no doubt that this approach leads to "less effective" and more consistent parameters. When we applied this approach to our data, we arrived at slightly better deviations for the infrared and submillimeter-wave data but the differences $|\nu_i(\text{exp}) - \nu_i(\text{calc})|$ were an order of magnitude larger for $J > 20$. For reasons described above and because primarily we wished to provide reliable experimental data rather than the final values of spectroscopic parameters in this paper, we have decided to present our data using standard weights $w_i(J) = (\Delta\sigma_i)^{-2}$.

TABLE IV
Parameters of the ν_6 Band of $^{12}\text{CH}_3\text{F}$ (in cm^{-1}) Taken from Table III

| Parameter | This work | Ref. (3) | Parameter | This work | Ref. (3) |
|-----------------------------|-------------------------------|------------------------------|------------------------------|----------------|---------------------------|
| ν_6 | 1182.674392 (17) ^a | 1182.67605 ^b (18) | $L_{JK} \times 10^{12}$ | -1.289 (118) | - |
| B_6 | 0.847883432 (162) | 0.847884295 (480) | $L_{KKJ} \times 10^{12}$ | 0.29 (43) | - |
| $D_J \times 10^6$ | 2.026360 (369) | 2.0552 (1398) | $\eta_J \times 10^6$ | 36.2953 (592) | 38.2398 (1514) |
| $D_{JK} \times 10^6$ | 15.37401 (1149) | 15.2522 (1409) | $\eta_K \times 10^6$ | 70.2924 (2436) | -320.2 ^a (220) |
| $D_K \times 10^6$ | 72.43491 (3332) | 70.315 ^b | $\tau_J \times 10^9$ | 2.887 (146) | |
| $H_J \times 10^{10}$ | 0.0026 (9) | -1.222 (218) | $\tau_{JK} \times 10^9$ | 17.812 (894) | |
| $H_{JK} \times 10^{10}$ | -1.580 (247) | 2.412 (2932) | $\tau_K \times 10^9$ | -10.688 (2157) | |
| $H_{KJ} \times 10^{10}$ | 1.684 (999) | -53.470 (11498) | $\sigma_J \times 10^{12}$ | -0.3044 (1022) | |
| $\Delta H_K \times 10^{10}$ | 0.866 (1734) | - | $\sigma_{JK} \times 10^{12}$ | 19.677 (1196) | |
| $(A_6 - B_6)$ | 4.35024130 (178) | 4.352715 ^b (1400) | $\sigma_{KJ} \times 10^{12}$ | -1.717 (2588) | |
| $2(A_6^2)_6$ | 3.08464144 (622) | 3.0874 ^b (22) | $q_{22} \times 10^6$ | -73.1603 (481) | 72.720 (330) |
| $L_{JJK} \times 10^{12}$ | 0.0408 (145) | - | $f_{22}^{(JJ)} \times 10^8$ | 1.80820 (637) | -1.7910 (215) |

^a Figures in parentheses are standard errors in units of the last digit quoted.

^b Constrained to the value given in Ref. (2); figures in parentheses are errors indicated in Ref. (2).

APPENDIX
TABLE A1Assignment of Observed Transitions in the ν_6 Band of $^{12}\text{CH}_3\text{F}$ (in cm^{-1})

| Line | Transition | Observed | Obs-Calc | Line | Transition | Observed | Obs-Calc | Line | Transition | Observed | Obs-Calc |
|------|-------------|-------------------|----------|------|-------------|-------------------|----------|------|------------|-------------------|----------|
| 1 | $p(2,1,1)$ | 107.345930 (-) | -3243 | 51 | $p(32,6)$ | 1092.427336 (-) | -200 | 101 | $p(23,7)$ | 1104.589171 (200) | 233 |
| 2 | $p(2,2,1)$ | 107.648981 (200) | 12 | 52 | $p(31,6)$ | 1093.017629 (200) | -380 | 102 | $p(24,6)$ | 1104.691218 (30) | 108 |
| 3 | $p(4,1,1)$ | 107.848704 (200) | -711 | 53 | $p(4,2,1)$ | 1093.250445 (200) | 92 | 103 | $p(25,6)$ | 1105.000000 (200) | 109 |
| 4 | $p(2,0,1)$ | 107.848704 (-) | -2333 | 54 | $p(4,1,2)$ | 1093.410894 (30) | 97 | 104 | $p(26,6)$ | 1105.242462 (200) | -694 |
| 5 | $p(4,2,1)$ | 107.969646 (-) | -5777 | 55 | $p(4,2,2)$ | 1093.463532 (200) | 48 | 105 | $p(27,6)$ | 1105.274519 (200) | -383 |
| 6 | $p(2,2,2)$ | 108.521215 (200) | -1277 | 56 | $p(4,3,1)$ | 1094.073578 (100) | 91 | 106 | $p(28,6)$ | 1105.427513 (30) | -133 |
| 7 | $p(4,0,1)$ | 108.680808 (200) | -817 | 57 | $p(4,3,2)$ | 1094.343758 (100) | -470 | 107 | $p(29,6)$ | 1105.700000 (200) | -306 |
| 8 | $p(4,0,2)$ | 108.680808 (200) | -999 | 58 | $p(4,4,1)$ | 1094.467096 (-) | 123 | 108 | $p(30,6)$ | 1105.868822 (200) | -149 |
| 9 | $p(2,2,0)$ | 108.738673 (1000) | -1382 | 59 | $p(4,3,1)$ | 1094.753304 (100) | -117 | 109 | $p(31,6)$ | 1105.863435 (30) | -316 |
| 10 | $p(2,0,2)$ | 108.738673 (330) | -1582 | 60 | $p(4,4,2)$ | 1094.759818 (100) | -101 | 110 | $p(32,6)$ | 1106.179781 (30) | -67 |
| 11 | $p(3,2,1)$ | 108.738673 (200) | 79 | 61 | $p(3,2,2)$ | 1095.159233 (200) | 310 | 111 | $p(33,6)$ | 1106.446532 (30) | 34 |
| 12 | $p(3,1,1)$ | 108.738673 (200) | -71 | 62 | $p(3,1,2)$ | 1095.213216 (100) | 226 | 112 | $p(34,6)$ | 1106.724661 (30) | 66 |
| 13 | $p(3,2,2)$ | 108.738673 (200) | -449 | 63 | $p(3,2,3)$ | 1095.307378 (100) | 266 | 113 | $p(35,6)$ | 1106.990504 (30) | 44 |
| 14 | $p(3,1,2)$ | 108.738673 (200) | -232 | 64 | $p(3,3,1)$ | 1096.283728 (100) | -393 | 114 | $p(36,6)$ | 1107.183333 (200) | -64 |
| 15 | $p(3,3,1)$ | 108.738673 (330) | -1362 | 65 | $p(3,3,2)$ | 1096.341028 (200) | -79 | 115 | $p(37,6)$ | 1107.212169 (200) | -339 |
| 16 | $p(3,2,0)$ | 108.738673 (200) | -472 | 66 | $p(3,4,1)$ | 1096.676500 (500) | 308 | 116 | $p(38,6)$ | 1107.435103 (30) | -68 |
| 17 | $p(3,3,2)$ | 108.738673 (200) | 105 | 67 | $p(3,4,2)$ | 1096.676500 (500) | -253 | 117 | $p(39,6)$ | 1107.495980 (200) | -465 |
| 18 | $p(3,0,1)$ | 108.738673 (200) | -271 | 68 | $p(3,4,3)$ | 1097.023227 (-) | -2617 | 118 | $p(40,6)$ | 1107.783269 (30) | -188 |
| 19 | $p(3,1,3)$ | 108.738673 (200) | -51 | 69 | $p(3,4,4)$ | 1097.435191 (100) | 215 | 119 | $p(41,6)$ | 1108.059648 (30) | -65 |
| 20 | $p(3,1,4)$ | 108.738673 (200) | -963 | 70 | $p(3,4,5)$ | 1097.435191 (100) | 215 | 120 | $p(42,6)$ | 1108.329326 (30) | -47 |
| 21 | $p(3,2,3)$ | 108.738673 (200) | -164 | 71 | $p(3,5,1)$ | 1097.800536 (30) | -168 | 121 | $p(43,6)$ | 1108.572335 (30) | 44 |
| 22 | $p(3,3,3)$ | 108.738673 (200) | -2331 | 72 | $p(3,5,2)$ | 1098.153900 (30) | 158 | 122 | $p(44,6)$ | 1108.812221 (30) | 86 |
| 23 | $p(3,2,4)$ | 108.738673 (200) | -157 | 73 | $p(3,5,3)$ | 1098.216980 (200) | -637 | 123 | $p(45,6)$ | 1109.033266 (30) | -128 |
| 24 | $p(3,3,4)$ | 108.738673 (200) | 232 | 74 | $p(3,5,4)$ | 1098.496531 (-) | -91 | 124 | $p(46,6)$ | 1109.161410 (80) | -338 |
| 25 | $p(3,4,1)$ | 108.738673 (200) | 232 | 75 | $p(3,5,5)$ | 1098.598000 (100) | -219 | 125 | $p(47,6)$ | 1109.161773 (100) | -410 |
| 26 | $p(3,4,2)$ | 108.738673 (200) | -261 | 76 | $p(3,6,1)$ | 1098.818295 (30) | -93 | 126 | $p(48,6)$ | 1109.400822 (30) | -328 |
| 27 | $p(3,4,3)$ | 108.738673 (200) | -1664 | 77 | $p(3,6,2)$ | 1098.957077 (200) | 15 | 127 | $p(49,6)$ | 1109.676685 (30) | -277 |
| 28 | $p(3,4,4)$ | 108.738673 (200) | 326 | 78 | $p(3,6,3)$ | 1099.310655 (30) | 84 | 128 | $p(50,6)$ | 1109.925453 (30) | -46 |
| 29 | $p(3,4,5)$ | 108.738673 (200) | 185 | 79 | $p(3,6,4)$ | 1099.654545 (30) | 132 | 129 | $p(51,6)$ | 1110.176455 (30) | 72 |
| 30 | $p(3,5,1)$ | 108.738673 (200) | 369 | 80 | $p(3,6,5)$ | 1099.780271 (30) | -560 | 130 | $p(52,6)$ | 1110.406290 (30) | 19 |
| 31 | $p(3,5,2)$ | 108.738673 (200) | 410 | 81 | $p(3,6,6)$ | 1099.985777 (30) | 96 | 131 | $p(53,6)$ | 1110.621339 (200) | -19 |
| 32 | $p(3,5,3)$ | 108.738673 (200) | 204 | 82 | $p(3,6,7)$ | 1100.143609 (100) | -653 | 132 | $p(54,6)$ | 1110.720202 (30) | -652 |
| 33 | $p(3,5,4)$ | 108.738673 (200) | -204 | 83 | $p(3,6,8)$ | 1100.305988 (100) | 82 | 133 | $p(55,6)$ | 1110.810984 (30) | -126 |
| 34 | $p(3,5,5)$ | 108.738673 (200) | -149 | 84 | $p(3,6,9)$ | 1100.498516 (30) | -35 | 134 | $p(56,6)$ | 1110.904899 (80) | -517 |
| 35 | $p(3,6,1)$ | 108.738673 (200) | -1057 | 85 | $p(3,6,10)$ | 1100.643645 (100) | 134 | 135 | $p(57,6)$ | 1111.064899 (80) | -385 |
| 36 | $p(3,6,2)$ | 108.738673 (200) | 314 | 86 | $p(3,6,11)$ | 1100.778158 (100) | 164 | 136 | $p(58,6)$ | 1111.363539 (30) | -312 |
| 37 | $p(3,6,3)$ | 108.738673 (200) | 314 | 87 | $p(3,6,12)$ | 1101.500854 (30) | 93 | 137 | $p(59,6)$ | 1111.562206 (30) | -168 |
| 38 | $p(3,6,4)$ | 108.738673 (200) | 158 | 88 | $p(3,6,13)$ | 1101.719097 (200) | -372 | 138 | $p(60,6)$ | 1111.796428 (30) | -59 |
| 39 | $p(3,6,5)$ | 108.738673 (200) | 143 | 89 | $p(3,6,14)$ | 1101.810544 (200) | -424 | 139 | $p(61,6)$ | 1112.021386 (30) | -5 |
| 40 | $p(3,6,6)$ | 108.738673 (200) | 81 | 90 | $p(3,6,15)$ | 1102.065598 (30) | -215 | 140 | $p(62,6)$ | 1112.230086 (30) | 78 |
| 41 | $p(3,6,7)$ | 108.738673 (200) | -789 | 91 | $p(3,6,16)$ | 1102.399146 (30) | -8 | 141 | $p(63,6)$ | 1112.423005 (30) | -77 |
| 42 | $p(3,6,8)$ | 108.738673 (200) | -63 | 92 | $p(3,6,17)$ | 1102.754252 (-) | -7 | 142 | $p(64,6)$ | 1112.570099 (200) | -436 |
| 43 | $p(3,6,9)$ | 108.738673 (200) | -562 | 93 | $p(3,6,18)$ | 1093.038249 (30) | 87 | 143 | $p(65,6)$ | 1112.810168 (80) | -457 |
| 44 | $p(3,6,10)$ | 108.738673 (200) | 95 | 94 | $p(3,6,19)$ | 1103.339681 (30) | 131 | 144 | $p(66,6)$ | 1113.041373 (30) | -337 |
| 45 | $p(3,6,11)$ | 108.738673 (200) | 366 | 95 | $p(3,6,20)$ | 1103.651016 (200) | -578 | 145 | $p(67,6)$ | 1113.242997 (30) | -148 |
| 46 | $p(3,6,12)$ | 108.738673 (200) | -2031 | 96 | $p(3,6,21)$ | 1103.900096 (200) | -64 | 146 | $p(68,6)$ | 1113.451373 (30) | -17 |
| 47 | $p(3,6,13)$ | 108.738673 (200) | -48 | 97 | $p(3,6,22)$ | 1104.195688 (100) | 42 | 147 | $p(69,6)$ | 1113.651373 (30) | -117 |
| 48 | $p(3,6,14)$ | 108.738673 (200) | -51 | 98 | $p(3,6,23)$ | 1104.490930 (30) | -56 | 148 | $p(70,6)$ | 1113.851373 (30) | 5 |
| 49 | $p(3,6,15)$ | 108.738673 (200) | 136 | 99 | $p(3,6,24)$ | 1104.790930 (30) | -215 | 149 | $p(71,6)$ | 1114.051373 (30) | -77 |
| 50 | $p(3,6,16)$ | 108.738673 (200) | -107 | 100 | $p(3,6,25)$ | 1105.051373 (30) | -107 | 150 | $p(72,6)$ | 1114.251373 (30) | -107 |

TABLE A1—Continued

| Line | Transition | Observed | Obs-Calc | Line | Transition | Observed | Obs-Calc | Line | Transition | Observed | Obs-Calc |
|------|--------------|-------------------|----------|------|---------------|-------------------|----------|------|---------------|------------------|----------|
| 251 | $\nu(1, 1)$ | 113.320205 (100) | 274 | 301 | $\nu(19, 2)$ | 1139.140663 (100) | -126 | 351 | $\nu(22, 0)$ | 1144.860339 (30) | -11 |
| 252 | $\nu(20, 0)$ | 113.320206 (200) | -60 | 302 | $\nu(22, 1)$ | 1139.140663 (30) | -116 | 352 | $\nu(22, 2)$ | 1144.860339 (30) | -43 |
| 253 | $\nu(21, 0)$ | 113.320206 (300) | -97 | 303 | $\nu(22, 3)$ | 1139.140663 (30) | -153 | 353 | $\nu(22, 4)$ | 1144.860339 (30) | -290 |
| 254 | $\nu(22, 0)$ | 113.320207 (1000) | -8 | 304 | $\nu(22, 5)$ | 1139.140663 (30) | -266 | 354 | $\nu(22, 6)$ | 1144.860339 (30) | -406 |
| 255 | $\nu(23, 0)$ | 113.320207 (200) | -367 | 305 | $\nu(22, 7)$ | 1139.140663 (30) | -583 | 355 | $\nu(22, 8)$ | 1144.860339 (30) | -900 |
| 256 | $\nu(24, 0)$ | 113.320207 (300) | -346 | 306 | $\nu(22, 9)$ | 1139.140663 (30) | -598 | 356 | $\nu(22, 10)$ | 1144.860339 (30) | -920 |
| 257 | $\nu(25, 0)$ | 113.320207 (400) | -380 | 307 | $\nu(22, 11)$ | 1139.140663 (30) | -958 | 357 | $\nu(22, 12)$ | 1144.860339 (30) | -1000 |
| 258 | $\nu(26, 0)$ | 113.320207 (500) | -406 | 308 | $\nu(22, 13)$ | 1139.140663 (30) | -1000 | 358 | $\nu(22, 14)$ | 1144.860339 (30) | -1020 |
| 259 | $\nu(27, 0)$ | 113.320207 (600) | -422 | 309 | $\nu(22, 15)$ | 1139.140663 (30) | -1040 | 359 | $\nu(22, 16)$ | 1144.860339 (30) | -1060 |
| 260 | $\nu(28, 0)$ | 113.320207 (700) | -446 | 310 | $\nu(22, 17)$ | 1139.140663 (30) | -1080 | 360 | $\nu(22, 18)$ | 1144.860339 (30) | -1100 |
| 261 | $\nu(29, 0)$ | 113.320207 (800) | -463 | 311 | $\nu(22, 19)$ | 1139.140663 (30) | -1120 | 361 | $\nu(22, 20)$ | 1144.860339 (30) | -1140 |
| 262 | $\nu(30, 0)$ | 113.320207 (900) | -489 | 312 | $\nu(22, 21)$ | 1139.140663 (30) | -1160 | 362 | $\nu(22, 22)$ | 1144.860339 (30) | -1180 |
| 263 | $\nu(31, 0)$ | 113.320207 (1000) | -511 | 313 | $\nu(22, 23)$ | 1139.140663 (30) | -1200 | 363 | $\nu(22, 24)$ | 1144.860339 (30) | -1220 |
| 264 | $\nu(32, 0)$ | 113.320207 (1100) | -541 | 314 | $\nu(22, 25)$ | 1139.140663 (30) | -1240 | 364 | $\nu(22, 26)$ | 1144.860339 (30) | -1260 |
| 265 | $\nu(33, 0)$ | 113.320207 (1200) | -570 | 315 | $\nu(22, 27)$ | 1139.140663 (30) | -1280 | 365 | $\nu(22, 28)$ | 1144.860339 (30) | -1300 |
| 266 | $\nu(34, 0)$ | 113.320207 (1300) | -600 | 316 | $\nu(22, 29)$ | 1139.140663 (30) | -1320 | 366 | $\nu(22, 30)$ | 1144.860339 (30) | -1340 |
| 267 | $\nu(35, 0)$ | 113.320207 (1400) | -630 | 317 | $\nu(22, 31)$ | 1139.140663 (30) | -1360 | 367 | $\nu(22, 32)$ | 1144.860339 (30) | -1380 |
| 268 | $\nu(36, 0)$ | 113.320207 (1500) | -660 | 318 | $\nu(22, 33)$ | 1139.140663 (30) | -1400 | 368 | $\nu(22, 34)$ | 1144.860339 (30) | -1420 |
| 269 | $\nu(37, 0)$ | 113.320207 (1600) | -690 | 319 | $\nu(22, 35)$ | 1139.140663 (30) | -1440 | 369 | $\nu(22, 36)$ | 1144.860339 (30) | -1460 |
| 270 | $\nu(38, 0)$ | 113.320207 (1700) | -720 | 320 | $\nu(22, 37)$ | 1139.140663 (30) | -1480 | 370 | $\nu(22, 38)$ | 1144.860339 (30) | -1500 |
| 271 | $\nu(39, 0)$ | 113.320207 (1800) | -750 | 321 | $\nu(22, 39)$ | 1139.140663 (30) | -1520 | 371 | $\nu(22, 40)$ | 1144.860339 (30) | -1540 |
| 272 | $\nu(40, 0)$ | 113.320207 (1900) | -780 | 322 | $\nu(22, 41)$ | 1139.140663 (30) | -1560 | 372 | $\nu(22, 42)$ | 1144.860339 (30) | -1580 |
| 273 | $\nu(41, 0)$ | 113.320207 (2000) | -810 | 323 | $\nu(22, 43)$ | 1139.140663 (30) | -1600 | 373 | $\nu(22, 44)$ | 1144.860339 (30) | -1620 |
| 274 | $\nu(42, 0)$ | 113.320207 (2100) | -840 | 324 | $\nu(22, 45)$ | 1139.140663 (30) | -1640 | 374 | $\nu(22, 46)$ | 1144.860339 (30) | -1660 |
| 275 | $\nu(43, 0)$ | 113.320207 (2200) | -870 | 325 | $\nu(22, 47)$ | 1139.140663 (30) | -1680 | 375 | $\nu(22, 48)$ | 1144.860339 (30) | -1700 |
| 276 | $\nu(44, 0)$ | 113.320207 (2300) | -900 | 326 | $\nu(22, 49)$ | 1139.140663 (30) | -1720 | 376 | $\nu(22, 50)$ | 1144.860339 (30) | -1740 |
| 277 | $\nu(45, 0)$ | 113.320207 (2400) | -930 | 327 | $\nu(22, 51)$ | 1139.140663 (30) | -1760 | 377 | $\nu(22, 52)$ | 1144.860339 (30) | -1780 |
| 278 | $\nu(46, 0)$ | 113.320207 (2500) | -960 | 328 | $\nu(22, 53)$ | 1139.140663 (30) | -1800 | 378 | $\nu(22, 54)$ | 1144.860339 (30) | -1820 |
| 279 | $\nu(47, 0)$ | 113.320207 (2600) | -990 | 329 | $\nu(22, 55)$ | 1139.140663 (30) | -1840 | 379 | $\nu(22, 56)$ | 1144.860339 (30) | -1860 |
| 280 | $\nu(48, 0)$ | 113.320207 (2700) | -1020 | 330 | $\nu(22, 57)$ | 1139.140663 (30) | -1880 | 380 | $\nu(22, 58)$ | 1144.860339 (30) | -1900 |
| 281 | $\nu(49, 0)$ | 113.320207 (2800) | -1050 | 331 | $\nu(22, 59)$ | 1139.140663 (30) | -1920 | 381 | $\nu(22, 60)$ | 1144.860339 (30) | -1940 |
| 282 | $\nu(50, 0)$ | 113.320207 (2900) | -1080 | 332 | $\nu(22, 61)$ | 1139.140663 (30) | -1960 | 382 | $\nu(22, 62)$ | 1144.860339 (30) | -1980 |
| 283 | $\nu(51, 0)$ | 113.320207 (3000) | -1110 | 333 | $\nu(22, 63)$ | 1139.140663 (30) | -2000 | 383 | $\nu(22, 64)$ | 1144.860339 (30) | -2020 |
| 284 | $\nu(52, 0)$ | 113.320207 (3100) | -1140 | 334 | $\nu(22, 65)$ | 1139.140663 (30) | -2040 | 384 | $\nu(22, 66)$ | 1144.860339 (30) | -2060 |
| 285 | $\nu(53, 0)$ | 113.320207 (3200) | -1170 | 335 | $\nu(22, 67)$ | 1139.140663 (30) | -2080 | 385 | $\nu(22, 68)$ | 1144.860339 (30) | -2100 |
| 286 | $\nu(54, 0)$ | 113.320207 (3300) | -1200 | 336 | $\nu(22, 69)$ | 1139.140663 (30) | -2120 | 386 | $\nu(22, 70)$ | 1144.860339 (30) | -2140 |
| 287 | $\nu(55, 0)$ | 113.320207 (3400) | -1230 | 337 | $\nu(22, 71)$ | 1139.140663 (30) | -2160 | 387 | $\nu(22, 72)$ | 1144.860339 (30) | -2180 |
| 288 | $\nu(56, 0)$ | 113.320207 (3500) | -1260 | 338 | $\nu(22, 73)$ | 1139.140663 (30) | -2200 | 388 | $\nu(22, 74)$ | 1144.860339 (30) | -2220 |
| 289 | $\nu(57, 0)$ | 113.320207 (3600) | -1290 | 339 | $\nu(22, 75)$ | 1139.140663 (30) | -2240 | 389 | $\nu(22, 76)$ | 1144.860339 (30) | -2260 |
| 290 | $\nu(58, 0)$ | 113.320207 (3700) | -1320 | 340 | $\nu(22, 77)$ | 1139.140663 (30) | -2280 | 390 | $\nu(22, 78)$ | 1144.860339 (30) | -2300 |
| 291 | $\nu(59, 0)$ | 113.320207 (3800) | -1350 | 341 | $\nu(22, 79)$ | 1139.140663 (30) | -2320 | 391 | $\nu(22, 80)$ | 1144.860339 (30) | -2340 |
| 292 | $\nu(60, 0)$ | 113.320207 (3900) | -1380 | 342 | $\nu(22, 81)$ | 1139.140663 (30) | -2360 | 392 | $\nu(22, 82)$ | 1144.860339 (30) | -2380 |
| 293 | $\nu(61, 0)$ | 113.320207 (4000) | -1410 | 343 | $\nu(22, 83)$ | 1139.140663 (30) | -2400 | 393 | $\nu(22, 84)$ | 1144.860339 (30) | -2420 |
| 294 | $\nu(62, 0)$ | 113.320207 (4100) | -1440 | 344 | $\nu(22, 85)$ | 1139.140663 (30) | -2440 | 394 | $\nu(22, 86)$ | 1144.860339 (30) | -2460 |
| 295 | $\nu(63, 0)$ | 113.320207 (4200) | -1470 | 345 | $\nu(22, 87)$ | 1139.140663 (30) | -2480 | 395 | $\nu(22, 88)$ | 1144.860339 (30) | -2500 |
| 296 | $\nu(64, 0)$ | 113.320207 (4300) | -1500 | 346 | $\nu(22, 89)$ | 1139.140663 (30) | -2520 | 396 | $\nu(22, 90)$ | 1144.860339 (30) | -2540 |
| 297 | $\nu(65, 0)$ | 113.320207 (4400) | -1530 | 347 | $\nu(22, 91)$ | 1139.140663 (30) | -2560 | 397 | $\nu(22, 92)$ | 1144.860339 (30) | -2580 |
| 298 | $\nu(66, 0)$ | 113.320207 (4500) | -1560 | 348 | $\nu(22, 93)$ | 1139.140663 (30) | -2600 | 398 | $\nu(22, 94)$ | 1144.860339 (30) | -2620 |
| 299 | $\nu(67, 0)$ | 113.320207 (4600) | -1590 | 349 | $\nu(22, 95)$ | 1139.140663 (30) | -2640 | 399 | $\nu(22, 96)$ | 1144.860339 (30) | -2660 |
| 300 | $\nu(68, 0)$ | 113.320207 (4700) | -1620 | 350 | $\nu(22, 97)$ | 1139.140663 (30) | -2680 | 400 | $\nu(22, 98)$ | 1144.860339 (30) | -2700 |

TABLE A1—Continued

| Line | Transition | Observed | Obs-Calc | Line | Transition | Observed | Obs-Calc | Line | Transition | Observed | Obs-Calc |
|------|------------|-------------------|----------|------|------------|-------------------|----------|------|------------|------------------|----------|
| 1001 | rk(13, 3) | 1206.97815 (200) | 25 | 1051 | rk(4, 4) | 1215.10366 (30) | 16 | 1101 | rk(17, 7) | 1222.95316 (100) | 9 |
| 1002 | rk(3, 3) | 1207.66469 (30) | 199 | 1052 | rk(26, 6) | 1215.14781 (100) | 254 | 1102 | rk(16, 5) | 1222.97991 (500) | -58 |
| 1003 | rk(1, 1) | 1207.70994 (2000) | -1395 | 1053 | rk(27, 6) | 1215.16466 (200) | 187 | 1103 | rk(16, 5) | 1222.98499 (500) | -64 |
| 1004 | rk(16, 9) | 1208.56870 (200) | -47 | 1054 | rk(26, 6) | 1215.174035 (200) | 146 | 1104 | rk(15, 7) | 1223.20972 (100) | 85 |
| 1005 | rk(7, 3) | 1208.59368 (100) | -61 | 1055 | rk(15, 1) | 1215.174035 (200) | 146 | 1105 | rk(4, 9) | 1223.20972 (100) | 85 |
| 1006 | rk(3, 3) | 1208.59368 (100) | -597 | 1056 | rk(26, 6) | 1215.174184 (30) | 127 | 1106 | rk(16, 5) | 1223.20972 (100) | 85 |
| 1007 | rk(3, 3) | 1208.59368 (100) | -597 | 1057 | rk(8, 3) | 1215.174184 (30) | 19 | 1107 | rk(15, 7) | 1223.20972 (100) | 85 |
| 1008 | rk(3, 3) | 1208.59368 (100) | -597 | 1058 | rk(26, 6) | 1215.174184 (30) | 142 | 1108 | rk(16, 5) | 1223.20972 (100) | 85 |
| 1009 | rk(29, 5) | 1209.10964 (30) | 473 | 1059 | rk(26, 6) | 1215.174184 (30) | 85 | 1109 | rk(15, 7) | 1223.20972 (100) | 85 |
| 1010 | rk(26, 6) | 1209.33568 (1000) | 382 | 1060 | rk(26, 6) | 1215.174184 (30) | 141 | 1110 | rk(16, 5) | 1223.20972 (100) | 85 |
| 1011 | rk(4, 3) | 1209.35875 (30) | 83 | 1061 | rk(26, 6) | 1215.174184 (30) | 142 | 1111 | rk(9, 7) | 1223.20972 (100) | 127 |
| 1012 | rk(1, 1) | 1209.37979 (30) | 106 | 1062 | rk(26, 6) | 1215.174184 (30) | 311 | 1112 | rk(16, 5) | 1223.20972 (100) | 85 |
| 1013 | rk(27, 3) | 1209.56262 (200) | -28 | 1063 | rk(16, 5) | 1215.174184 (30) | -1086 | 1113 | rk(15, 7) | 1223.20972 (100) | 85 |
| 1014 | rk(15, 1) | 1209.56262 (200) | -28 | 1064 | rk(16, 5) | 1215.174184 (30) | 60 | 1114 | rk(16, 5) | 1223.20972 (100) | 85 |
| 1015 | rk(26, 6) | 1209.56262 (200) | -28 | 1065 | rk(16, 5) | 1215.174184 (30) | 60 | 1115 | rk(16, 5) | 1223.20972 (100) | 85 |
| 1016 | rk(26, 6) | 1209.56262 (200) | -28 | 1066 | rk(16, 5) | 1215.174184 (30) | 60 | 1116 | rk(16, 5) | 1223.20972 (100) | 85 |
| 1017 | rk(15, 1) | 1210.13680 (200) | 111 | 1067 | rk(16, 5) | 1215.174184 (30) | 39 | 1117 | rk(16, 5) | 1223.20972 (100) | 85 |
| 1018 | rk(26, 6) | 1210.13680 (200) | 233 | 1068 | rk(16, 5) | 1215.174184 (30) | 20 | 1118 | rk(16, 5) | 1223.20972 (100) | 85 |
| 1019 | rk(8, 3) | 1210.22589 (100) | 210 | 1069 | rk(16, 5) | 1215.174184 (30) | 77 | 1119 | rk(16, 5) | 1223.20972 (100) | 85 |
| 1020 | rk(26, 6) | 1210.22589 (100) | 210 | 1070 | rk(16, 5) | 1215.174184 (30) | 42 | 1120 | rk(16, 5) | 1223.20972 (100) | 85 |
| 1021 | rk(22, 5) | 1210.52496 (100) | 209 | 1071 | rk(16, 5) | 1215.174184 (30) | 20 | 1121 | rk(16, 5) | 1223.20972 (100) | 85 |
| 1022 | rk(26, 6) | 1210.52496 (100) | 103 | 1072 | rk(16, 5) | 1215.174184 (30) | 47 | 1122 | rk(16, 5) | 1223.20972 (100) | 85 |
| 1023 | rk(26, 6) | 1210.52496 (100) | 93 | 1073 | rk(16, 5) | 1215.174184 (30) | 6 | 1123 | rk(16, 5) | 1223.20972 (100) | 85 |
| 1024 | rk(12, 1) | 1210.96686 (500) | 140 | 1074 | rk(16, 5) | 1215.174184 (30) | 55 | 1124 | rk(16, 5) | 1223.20972 (100) | 85 |
| 1025 | rk(19, 5) | 1211.01682 (2000) | 3210 | 1075 | rk(16, 5) | 1215.174184 (30) | 66 | 1125 | rk(16, 5) | 1223.20972 (100) | 85 |
| 1026 | rk(15, 3) | 1211.01682 (2000) | -95 | 1076 | rk(16, 5) | 1215.174184 (30) | 115 | 1126 | rk(16, 5) | 1223.20972 (100) | 85 |
| 1027 | rk(16, 5) | 1211.01682 (2000) | 115 | 1077 | rk(16, 5) | 1215.174184 (30) | 33 | 1127 | rk(16, 5) | 1223.20972 (100) | 85 |
| 1028 | rk(12, 1) | 1211.20846 (30) | 2 | 1078 | rk(16, 5) | 1215.174184 (30) | 141 | 1128 | rk(16, 5) | 1223.20972 (100) | 85 |
| 1029 | rk(16, 5) | 1211.20846 (30) | 45 | 1079 | rk(16, 5) | 1215.174184 (30) | 76 | 1129 | rk(16, 5) | 1223.20972 (100) | 85 |
| 1030 | rk(15, 5) | 1211.52459 (30) | 39 | 1080 | rk(16, 5) | 1215.174184 (30) | -77 | 1130 | rk(16, 5) | 1223.20972 (100) | 85 |
| 1031 | rk(16, 5) | 1211.67080 (30) | 61 | 1081 | rk(16, 5) | 1215.174184 (30) | -24 | 1131 | rk(16, 5) | 1223.20972 (100) | 85 |
| 1032 | rk(15, 5) | 1211.67080 (30) | 41 | 1082 | rk(16, 5) | 1215.174184 (30) | -14 | 1132 | rk(16, 5) | 1223.20972 (100) | 85 |
| 1033 | rk(15, 5) | 1211.67080 (30) | 46 | 1083 | rk(16, 5) | 1215.174184 (30) | -14 | 1133 | rk(16, 5) | 1223.20972 (100) | 85 |
| 1034 | rk(15, 5) | 1211.67080 (30) | -86 | 1084 | rk(16, 5) | 1215.174184 (30) | -63 | 1134 | rk(16, 5) | 1223.20972 (100) | 85 |
| 1035 | rk(15, 5) | 1211.67080 (30) | -29 | 1085 | rk(16, 5) | 1215.174184 (30) | -16 | 1135 | rk(16, 5) | 1223.20972 (100) | 85 |
| 1036 | rk(15, 5) | 1211.67080 (30) | -34 | 1086 | rk(16, 5) | 1215.174184 (30) | -109 | 1136 | rk(16, 5) | 1223.20972 (100) | 85 |
| 1037 | rk(15, 5) | 1211.67080 (30) | 10 | 1087 | rk(16, 5) | 1215.174184 (30) | -659 | 1137 | rk(16, 5) | 1223.20972 (100) | 85 |
| 1038 | rk(15, 5) | 1211.67080 (30) | 29 | 1088 | rk(16, 5) | 1215.174184 (30) | 586 | 1138 | rk(16, 5) | 1223.20972 (100) | 85 |
| 1039 | rk(15, 5) | 1211.67080 (30) | 29 | 1089 | rk(16, 5) | 1215.174184 (30) | -859 | 1139 | rk(16, 5) | 1223.20972 (100) | 85 |
| 1040 | rk(15, 5) | 1211.67080 (30) | -10 | 1090 | rk(16, 5) | 1215.174184 (30) | 110 | 1140 | rk(16, 5) | 1223.20972 (100) | 85 |
| 1041 | rk(15, 5) | 1211.67080 (30) | 124 | 1091 | rk(16, 5) | 1215.174184 (30) | 80 | 1141 | rk(16, 5) | 1223.20972 (100) | 85 |
| 1042 | rk(15, 5) | 1211.67080 (30) | -22 | 1092 | rk(16, 5) | 1215.174184 (30) | 169 | 1142 | rk(16, 5) | 1223.20972 (100) | 85 |
| 1043 | rk(15, 5) | 1211.67080 (30) | -44 | 1093 | rk(16, 5) | 1215.174184 (30) | -99 | 1143 | rk(16, 5) | 1223.20972 (100) | 85 |
| 1044 | rk(15, 5) | 1211.67080 (30) | -36 | 1094 | rk(16, 5) | 1215.174184 (30) | -99 | 1144 | rk(16, 5) | 1223.20972 (100) | 85 |
| 1045 | rk(15, 5) | 1211.67080 (30) | -71 | 1095 | rk(16, 5) | 1215.174184 (30) | -99 | 1145 | rk(16, 5) | 1223.20972 (100) | 85 |
| 1046 | rk(15, 5) | 1211.67080 (30) | -52 | 1096 | rk(16, 5) | 1215.174184 (30) | 105 | 1146 | rk(16, 5) | 1223.20972 (100) | 85 |
| 1047 | rk(15, 5) | 1211.67080 (30) | -52 | 1097 | rk(16, 5) | 1215.174184 (30) | 32 | 1147 | rk(16, 5) | 1223.20972 (100) | 85 |
| 1048 | rk(15, 5) | 1211.67080 (30) | -52 | 1098 | rk(16, 5) | 1215.174184 (30) | 91 | 1148 | rk(16, 5) | 1223.20972 (100) | 85 |
| 1049 | rk(15, 5) | 1211.67080 (30) | -278 | 1099 | rk(16, 5) | 1215.174184 (30) | -45 | 1149 | rk(16, 5) | 1223.20972 (100) | 85 |
| 1050 | rk(15, 5) | 1211.67080 (30) | 34 | 1100 | rk(16, 5) | 1215.174184 (30) | -40 | 1150 | rk(16, 5) | 1223.20972 (100) | 85 |
| 1051 | rk(15, 5) | 1211.67080 (30) | -124 | 1101 | rk(16, 5) | 1215.174184 (30) | 80 | 1151 | rk(16, 5) | 1223.20972 (100) | 85 |
| 1052 | rk(15, 5) | 1211.67080 (30) | -124 | 1102 | rk(16, 5) | 1215.174184 (30) | 80 | 1152 | rk(16, 5) | 1223.20972 (100) | 85 |
| 1053 | rk(15, 5) | 1211.67080 (30) | -124 | 1103 | rk(16, 5) | 1215.174184 (30) | 80 | 1153 | rk(16, 5) | 1223.20972 (100) | 85 |
| 1054 | rk(15, 5) | 1211.67080 (30) | -124 | 1104 | rk(16, 5) | 1215.174184 (30) | 80 | 1154 | rk(16, 5) | 1223.20972 (100) | 85 |
| 1055 | rk(15, 5) | 1211.67080 (30) | -124 | 1105 | rk(16, 5) | 1215.174184 (30) | 80 | 1155 | rk(16, 5) | 1223.20972 (100) | 85 |
| 1056 | rk(15, 5) | 1211.67080 (30) | -124 | 1106 | rk(16, 5) | 1215.174184 (30) | 80 | 1156 | rk(16, 5) | 1223.20972 (100) | 85 |
| 1057 | rk(15, 5) | 1211.67080 (30) | -124 | 1107 | rk(16, 5) | 1215.174184 (30) | 80 | 1157 | rk(16, 5) | 1223.20972 (100) | 85 |
| 1058 | rk(15, 5) | 1211.67080 (30) | -124 | 1108 | rk(16, 5) | 1215.174184 (30) | 80 | 1158 | rk(16, 5) | 1223.20972 (100) | 85 |
| 1059 | rk(15, 5) | 1211.67080 (30) | -124 | 1109 | rk(16, 5) | 1215.174184 (30) | 80 | 1159 | rk(16, 5) | 1223.20972 (100) | 85 |
| 1060 | rk(15, 5) | 1211.67080 (30) | -124 | 1110 | rk(16, 5) | 1215.174184 (30) | 80 | 1160 | rk(16, 5) | 1223.20972 (100) | 85 |

Notes:

Numbers in parentheses represent estimated experimental uncertainties in units of the last digit quoted. Asterisks denote experimental data which have not been included in the fit. The Obs-Calc values are given in the same units as experimental uncertainties.

TABLE A2

Comparison of Observed and Calculated Transition Frequencies of Purely Rotational Transitions in the $\nu_6 = 1$ State of $^{12}\text{CH}_3\text{F}$ (in MHz)

| J | kl | Exp | Calc | Exp-Calc | J | kl | Exp | Calc | Exp-Calc |
|---|----|------------------|-----------|----------|----|----|------------------|-----------|----------|
| 0 | 0 | 50837.75 (20)A | 50837.57 | 18 | 6 | 1 | 355850.44 (20) | 355850.16 | 28 |
| | | | | | 6 | 2 | 355786.31 (20) | 355786.34 | -3 |
| 1 | 0 | 101673.77 (20)B | 101673.68 | 9 | 6 | 3 | 355769.66 (20) | 355769.51 | 15 |
| 1 | 1 | 101659.03 (20)B | 101658.68 | 35 | 6 | 4 | 355740.07 (20) | 355739.94 | 14 |
| 1 | 1 | 101693.87 (20)B | 101693.71 | 17 | 6 | 5 | 355697.73 (20) | 355697.64 | 9 |
| 1 | -1 | 101667.40 (20)B | 101667.48 | -8 | 6 | 6 | 355642.77 (20) | 355642.68 | 9 |
| | | | | | 6 | -1 | 355759.46 (20) | 355759.40 | -2 |
| 2 | 0 | 152506.86 (10)C | 152506.87 | -0 | 6 | -2 | 355724.69 (20) | 355724.72 | -3 |
| 2 | 1 | 152484.32 (10)C | 152484.45 | -12 | 6 | -3 | 355676.81 (20) | 355676.95 | -14 |
| 2 | 1 | 152536.99 (10)C | 152536.85 | 14 | 6 | -4 | 355615.94 (20) | 355616.14 | -20 |
| 2 | 2 | 152508.97 (10)C | 152508.92 | 5 | 6 | -5 | 355542.13 (20) | 355542.24 | -11 |
| 2 | -1 | 152497.55 (10)C | 152497.56 | -2 | 6 | -6 | 355455.21 (20) | 355455.22 | -1 |
| 2 | -2 | 152482.66 (10)C | 152482.71 | -5 | | | | | |
| | | | | | 7 | 0 | 406578.13 (20)C | 406577.97 | 16 |
| 3 | 0 | 203335.71 (10)C | 203335.68 | 3 | 7 | 1 | 406520.22 (20) | 406520.33 | -11 |
| 3 | 1 | 203305.84 (10) | 203305.92 | -9 | 7 | 1 | 406656.53 (20) | 406656.26 | 27 |
| 3 | 1 | 203375.75 (20) | 203375.55 | 20 | 7 | 2 | 406584.04 (20)C | 406583.90 | 14 |
| 3 | 2 | 203338.54 (20) | 203338.45 | 10 | 7 | 3 | 406564.89 (20) | 406564.69 | 20 |
| 3 | 3 | 203328.86 (20) | 203328.81 | 5 | 7 | 4 | 406531.00 (20) | 406530.91 | 9 |
| 3 | -1 | 203323.28 (20) | 203323.27 | 1 | 7 | 5 | 406482.79 (20) | 406482.60 | 19 |
| 3 | -2 | 203303.46 (10)C | 203303.45 | 0 | 7 | 6 | 406419.96 (20) | 406419.81 | 16 |
| 3 | -3 | 203276.14 (10)C | 203276.21 | -7 | 7 | 7 | 406342.61 (20) | 406342.59 | 2 |
| | | | | | 7 | -1 | 406552.93 (20)C | 406553.05 | -12 |
| 4 | 0 | - | 254158.66 | | 7 | -2 | 406513.71 (200) | 406513.28 | 43 |
| 4 | 1 | 254123.50 (300) | 254121.68 | 182 | 7 | -3 | 406458.49 (20) | 406458.64 | -15 |
| 4 | 1 | 254209.11 (300) | 254208.33 | 78 | 7 | -4 | 406388.87 (20) | 406389.09 | -22 |
| 4 | 2 | 254161.98 (20) | 254162.16 | -18 | 7 | -5 | 406304.39 (20) | 406304.58 | -19 |
| 4 | 3 | 254150.24 (20) | 254150.12 | 12 | 7 | -6 | 406204.92 (20) | 406205.07 | -15 |
| 4 | 4 | 254129.07 (20) | 254128.97 | 10 | 7 | -7 | 406090.13 (100) | 406090.52 | -39 |
| 4 | -1 | - | 254143.13 | | | | | | |
| 4 | -2 | 254118.44 (20) | 254118.34 | 10 | 8 | 0 | - | 457363.01 | |
| 4 | -3 | 254084.26 (20) | 254084.27 | -1 | 8 | 1 | - | 457298.90 | |
| 4 | -4 | 254040.84 (20) | 254040.88 | -4 | 8 | 1 | 457450.72 (20) | 457450.50 | 22 |
| | | | | | 8 | 2 | - | 457369.84 | |
| 5 | 0 | - | 304974.34 | | 8 | 3 | 457348.44 (20) | 457348.25 | 19 |
| 5 | 1 | 304932.55 (300) | 304930.28 | 227 | 8 | 4 | - | 457310.28 | |
| 5 | 1 | 305033.92 (20) | 305033.69 | 23 | 8 | 5 | 457256.20 (20) | 457255.96 | 24 |
| 5 | 2 | 304978.77 (20) | 304978.61 | 16 | 8 | 6 | 457185.46 (20) | 457185.34 | 12 |
| 5 | 3 | 304964.31 (20) | 304964.17 | 14 | 8 | 7 | 457098.53 (100) | 457098.50 | 3 |
| 5 | 4 | 304938.94 (20) | 304938.80 | 14 | 8 | 8 | - | 456995.50 | |
| 5 | 5 | 304902.72 (20) | 304902.54 | 18 | 8 | -1 | 457334.96 (20) | 457334.93 | 3 |
| 5 | -1 | 304955.68 (20) | 304955.69 | -1 | 8 | -2 | - | 457290.14 | |
| 5 | -2 | - | 304925.92 | | 8 | -3 | 457228.39 (20) | 457228.61 | -22 |
| 5 | -3 | 304884.88 (20)C | 304885.01 | -12 | 8 | -4 | 457150.00 (20) | 457150.29 | -29 |
| 5 | -4 | 304832.82 (20) | 304832.91 | -9 | 8 | -5 | 457054.79 (20) | 457055.15 | -36 |
| 5 | -5 | 304769.58 (20) | 304769.61 | -3 | 8 | -6 | 456942.76 (200) | 456943.13 | -37 |
| | | | | | 8 | -7 | 456813.86 (200) | 456814.18 | -32 |
| 6 | 0 | 355781.36 (20) | 355781.26 | 10 | 8 | -8 | 456668.01 (200) | 456668.27 | -26 |
| 6 | 1 | 355730.07 (20) | 355730.31 | -24 | | | | | |
| | | | | | | | | | |
| 9 | 0 | - | 508134.91 | | 10 | -1 | 558858.95 (20) | 558857.80 | 115 |
| 9 | 1 | 508064.43 (20) | 508064.61 | -18 | 10 | -2 | 558804.83 (-)* | 558802.90 | 193 |
| 9 | 1 | 508231.62 (20) | 508231.40 | 22 | 10 | -3 | 558728.46 (20) | 558727.52 | 94 |
| 9 | 2 | 508142.54 (20) | 508142.70 | -16 | 10 | -4 | 558632.29 (20) | 558631.61 | 68 |

Our measurement unless stated otherwise: A(18), B(19), C(17). The J and kl values refer to quantum numbers of the lower state of the rotational transition. Numbers in parentheses represent estimated experimental uncertainties in units of the last digit quoted. Asterisks denote experimental data which have not included in the fit. The Exp-Calc values are given in the same units as experimental uncertainties.

TABLE A2—Continued

| J | kl | Exp | Calc | Exp-Calc | J | kl | Exp | Calc | Exp-Calc |
|----|----|------------------|-----------|----------|----|-----|------------------|-----------|----------|
| 9 | 3 | 508118.91 (20) | 508118.74 | 17 | 10 | -5 | 558515.67 (20) | 558515.12 | 55 |
| 9 | 4 | - | 508076.59 | | 10 | -6 | 558377.83 (20) | 558377.98 | -15 |
| 9 | 5 | 508016.48 (20) | 508016.27 | 21 | 10 | -7 | 558219.11 (20) | 558220.15 | -104 |
| 9 | 6 | 507938.04 (20) | 507937.84 | 20 | 10 | -8 | 558040.15 (20) | 558041.58 | -143 |
| 9 | 7 | 507841.48 (20) | 507841.38 | 11 | 10 | -9 | 557840.54 (200) | 557842.20 | -166 |
| 9 | 8 | 507726.96 (20) | 507726.96 | 1 | 10 | -10 | - | 557621.97 | |
| 9 | 9 | 507595.61 (200) | 507594.66 | 95 | | | | | |
| 9 | -1 | 508103.56 (20) | 508103.67 | -11 | 11 | 0 | 609633.73 (20) | 609633.49 | 24 |
| 9 | -2 | 508053.86 (20) | 508053.83 | 3 | 11 | 1 | 609551.69 (20) | 609551.69 | 0 |
| 9 | -3 | 507985.07 (20) | 507985.39 | -32 | 11 | 1 | 609746.69 (20) | 609747.26 | -57 |
| 9 | -4 | 507897.89 (20) | 507898.29 | -40 | 11 | 2 | 609643.10 (20) | 609643.36 | -27 |
| 9 | -5 | 507792.04 (20) | 507792.49 | -45 | 11 | 3 | 609614.96 (20) | 609614.71 | 25 |
| 9 | -6 | 507667.35 (20) | 507667.92 | -57 | 11 | 4 | 609564.41 (20) | 609564.24 | 17 |
| 9 | -7 | 507523.75 (20) | 507524.55 | -80 | 11 | 5 | 609492.29 (20) | 609491.95 | 34 |
| 9 | -8 | 507361.41 (200) | 507362.32 | -91 | 11 | 6 | 609398.33 (20) | 609397.93 | 40 |
| 9 | -9 | 507180.07 (20) | 507181.19 | -112 | 11 | 7 | 609282.60 (20) | 609282.25 | 35 |
| | | | | | 11 | 8 | 609145.36 (20) | 609145.00 | 35 |
| 10 | 0 | 558896.86 (-)* | 558892.23 | 463 | 11 | 9 | 608986.77 (20) | 608986.29 | 47 |
| 10 | 1 | - | 558816.02 | | 11 | 10 | 608806.42 (20) | 608806.22 | 20 |
| 10 | 1 | 558998.67 (20) | 558997.48 | 119 | 11 | -1 | 609595.70 (20) | 609595.87 | -17 |
| 10 | 2 | - | 558901.02 | | 11 | -2 | 609536.20 (100) | 609535.88 | 33 |
| 10 | 3 | 558876.10 (20) | 558874.71 | 139 | 11 | -3 | 609453.08 (20) | 609453.53 | -45 |
| 10 | 4 | 558828.46 (20) | 558828.39 | 7 | 11 | -4 | 609348.18 (20) | 609348.79 | -60 |
| 10 | 5 | 558763.83 (20) | 558762.08 | 175 | 11 | -5 | 609220.81 (20) | 609221.57 | -76 |
| 10 | 6 | 558677.20 (20) | 558675.85 | 135 | 11 | -6 | 609070.75 (20) | 609071.84 | -108 |
| 10 | 7 | 558571.13 (20) | 558569.77 | 136 | 11 | -7 | 608898.01 (20) | 608899.51 | -151 |
| 10 | 8 | 558445.07 (20) | 558443.94 | 113 | 11 | -8 | 608702.39 (20) | 608704.55 | -215 |
| 10 | 9 | 558300.30 (200) | 558298.43 | 187 | 11 | -9 | 608483.87 (200) | 608486.88 | -301 |
| 10 | 10 | 558133.73 (200) | 558133.35 | 38 | 11 | -10 | 608235.63 (-)* | 608246.46 | -1083 |

ACKNOWLEDGMENTS

We are indebted to Dr. R. Fajgar and Dr. M. Horák (Prague) for help in preparing the sample of $^{12}\text{CH}_3\text{F}$ and Klaus Lattner (Giessen) for his expert help in obtaining the FT-IR spectra. The laboratory work carried out in Giessen was supported in part by the Deutsche Forschungsgemeinschaft and the Fonds der Chemischen Industrie. We thank Dr. B. P. Winnewisser for her help with the manuscript.

RECEIVED: December 19, 1990

REFERENCES

1. W. L. SMITH AND I. M. MILLS, *J. Mol. Spectrosc.* **11**, 11–38 (1963).
2. E. HIROTA, *J. Mol. Spectrosc.* **74**, 209–216 (1979).
3. HANG-G. CHO, Y. MATSUO, AND R. H. SCHWENDEMAN, *J. Mol. Spectrosc.* **137**, 215–229 (1989).
4. M. BIRK, M. WINNEWISSER, AND E. A. COHEN, *J. Mol. Spectrosc.* **136**, 402–445 (1989).
5. S. P. BELOV, A. V. BURENIN, L. I. GERSHTEIN, V. V. KOROLIKHIN, AND A. F. KRUPNOV, *Opt. Spectrosc.* **35**, 295–302 (1974).
6. Š. URBAN, D. PAPOUŠEK, AND M. GARCIA HERNANDEZ, *J. Mol. Spectrosc.* **124**, 272–284 (1987).
7. K. SARKA AND D. PAPOUŠEK, *Mol. Phys.* **65**, 829–841 (1988).
8. E. I. LOBODENKO, O. N. SULAKSHINA, V. I. PEREVALOV, AND V. G. TYUTEREV, *J. Mol. Spectrosc.* **126**, 159–170 (1987).

9. SANG K. LEE, R. H. SCHWENDEMAN, R. L. CROWNOVER, D. D. SKATRUND, AND F. C. DELUCIA, *J. Mol. Spectrosc.* **123**, 145–160 (1987).
10. J. R. IZATT, B. K. DEKA, AND WEN-SEN ZHU, *IEEE J. Quantum Electron.* **QE23**, 117–122 (1987).
11. W. F. EDGELL AND L. PARTS, *J. Am. Chem. Soc.* **77**, 4899–4902 (1955).
12. G. GUELACHVILI AND K. NARAHARI RAO, "Handbook of Infrared Standards," Academic Press, Orlando/London/New York/Tokyo, 1986.
13. K. SARKA, *J. Mol. Spectrosc.* **41**, 233–239 (1972).
14. G. DI LONARDO, L. FUSINA, AND J. W. C. JOHNS, *J. Mol. Spectrosc.* **104**, 282–301 (1984).
15. R. S. WINTON AND W. GORDY, *Phys. Lett. A* **32**, 219–220 (1970).
16. D. BOUCHER, J. BURIE, R. BOCQUET, AND J. DEMAISON, *J. Mol. Spectrosc.* **116**, 256–258 (1986).
17. F. X. BROWN, D. DANGOISE, J. GADLIE, . WLODARCZAK, AND J. DEMAISON, *J. Mol. Struct.* **190**, 401–407 (1988).
18. T. TANAKA AND E. HIROTA, *J. Mol. Spectrosc.* **54**, 437–446 (1975).
19. E. HIROTA, T. TANAKA, AND S. SAITO, *J. Mol. Spectrosc.* **63**, 478–484 (1976).
20. D. PAPOUŠEK, P. PRACNA, R. TESAŘ, S. P. BELOV, AND M. YU. TRETYAKOV, *Vib. Spectros.*, in print.
21. G. GRANER, *Mol. Phys.* **31**, 1833–1843 (1976).
22. P. PRACNA, D. PAPOUŠEK, S. P. BELOV, M. YU. TRETYAKOV, AND K. SARKA, *J. Mol. Spectrosc.*, in print.
23. M. BADAQUI AND J. P. CHAMPION, *J. Mol. Spectrosc.* **109**, 402–411 (1985).